Analytical Modeling of Forced Convection in Slotted Plate Fin Heat Sinks

P. Teertstra*, J.R. Culham† and M.M. Yovanovich‡

Microelectronics Heat Transfer Laboratory
Department of Mechanical Engineering
University of Waterloo
Waterloo, Ontario, Canada

ABSTRACT

Analytical models are developed for the average heat transfer rate in forced convection-cooled, slotted fin heat sinks. These models for the upper and lower bounds can be used to investigate the effects of slot size and placement on heat sink performance. Experimental measurements are performed for a variety of slot configurations over a range of Reynolds numbers, and these data are compared with the proposed analytical models. An approximate model is proposed that predicts the experimental results for the average heat transfer rate to within a 12% RMS difference.

NOMENCLATURE

A	=	channel surface area, m^2
A_a	=	approach flow cross section area, m^2
A_o	=	heat sink flow cross section area, m^2
b	=	channel spacing, m
g	=	gravitational acceleration (m/s^2)
h	=	average heat transfer coefficient, W/m^2K
H	=	fin height, m
k	=	fin thermal conductivity, W/mK
k_f	=	fluid thermal conductivity, W/mK
L	=	baseplate length, m
$\dot{m}$	=	mass flow rate, kg/s
n	=	composite model combination parameter
N	=	number of fins
N_s	=	number of slots
Nu_b	=	Nusselt number, $\equiv (Qb)/(k_f A \Delta T)$
Nu_i	=	ideal Nusselt number, $\eta = 1$
P	=	slot pitch, m
Pr	=	Prandtl number, $\equiv \nu/\alpha$
Q	=	total heat transfer rate, W
R	=	thermal resistance, $\equiv 1/h\,A$, $^oC/W$
Re_b	=	Reynolds number, $\equiv Ub/\nu$
$Re_b^\star$	=	channel Reynolds number, $\equiv Re_b \cdot (b/L)$
S	=	slot width, m
T_a	=	inlet air temperature, ^oC
T_f	=	film temperature, $\equiv (T_s + T_a)/2$, ^oC
T_s	=	baseplate temperature, ^oC
ΔT	=	temperature difference, $\equiv T_s - T_a$, ^oC
t	=	fin thickness, m
U	=	average velocity in channel, m/s
U_a	=	approach velocity, m/s
W	=	baseplate width, m

Greek Symbols

α	=	thermal diffusivity (m^2/s)
β	=	thermal expansion coefficient $(1/K)$
η	=	fin efficiency, $\equiv Nu_b/Nu_i$
ν	=	kinematic viscosity (m^2/s)

Subscripts

dev	=	developing
fd	=	fully developed
LB	=	lower bound
UB	=	upper bound

* Graduate Research Assistant
† Research Associate Professor and Member, ASME
‡ Professor and Fellow, ASME

INTRODUCTION

Finned heat sinks are commonly used for enhancing heat transfer in air-cooled microelectronics and power electronics applications. The use of finned heat sinks reduces the thermal resistance and operating temperatures of components and assemblies by increasing the available surface area for convective heat transfer. The plate fin heat shown in Fig. 1a) is one of the most common heat sink configurations used in current applications, consisting of a parallel array of thin flat plates attached to a single, thermally conductive baseplate. Forced convection heat transfer occurs in the channels formed between adjacent fins by fan or blower-driven airflow in a direction parallel to the baseplate.

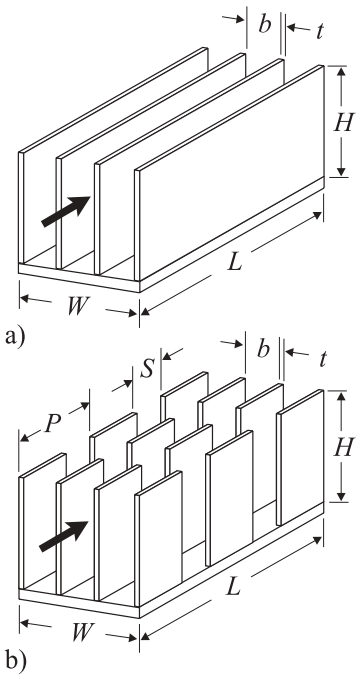

Figure 1: Schematic of Heat Sink Geometry
a) Plate Fin Heat Sink
b) Slotted Plate Fin Heat Sink

An enhancement of the thermal performance of plate fin heat sinks achieved through the introduction of slotted sections in the fin surfaces has been proposed (R-Theta, 1999), as shown in Fig. 1b). Placing slots in the fins at regular intervals causes new thermal boundary layers to be initiated at each fin section, resulting in a reduction of the average boundary layer thickness and an increase in the average heat transfer coefficient. However, these slots also contribute to a decrease in the available surface area for convection, which may reduce the total heat transfer from the heat sink. An optimal slotted plate fin heat sink design is one that balances the enhancement in the heat transfer coefficient with the subsequent reduction in surface area.

In order to optimize all the heat sink parameters, including the relative size and placement of slots, analytical models are required that predict heat sink thermal performance as a function of slot geometry and overall fin area. These analytical design tools can be used for parametric and trade-off studies early in the design process, prior to more costly and time consuming numerical simulations or prototype testing. There are no models or correlations currently available in the literature for slotted fin heat sinks, and no experimental or numerical results have been presented that address this problem.

The objective of the current study is to develop analytical models for the average heat transfer rate of slotted fin heat sinks for the full range of Re from fully developed to laminar developing flow. The proposed models will include fin effects to account for the variation in fin temperature, an important factor in the high aspect ratio heat sinks examined in this study. Experimental measurements will examine the performance of various slotted heat sink configurations as a function of slot size and spacing, and these data will be used to validate the proposed models.

MODEL DEVELOPMENT

Problem Description

The problem of interest in this research study involves forced convection heat transfer from air-cooled plate fin heat sinks with slotted fins, as shown in Fig. 1b). The heat sink consists of a parallel array of N fins of thermal conductivity k attached to a rectangular baseplate, with dimensions as shown in Fig. 1. The baseplate is assumed to be relatively thick with a large value of thermal conductivity, such that spreading resistance can be neglected and the baseplate can be treated as isothermal. The lower surface and edges of the baseplate are assumed to be adiabatic, such that all heat transferred by the heat sink is dissipated from the fins by convection.

The slotted fin heat sinks consist of uniformly sized and spaced slots cut into the fins from the fin tip to the baseplate, such that the remaining fin sections are separated from each other and connected only by the baseplate. The size and spacing of the slots can be fully described by two geometric parameters as shown in Fig. 2, the slot pitch P, and the slot width S. For the subsequent analysis, it is convenient to nondimensionalize the slot pitch by the baseplate length,

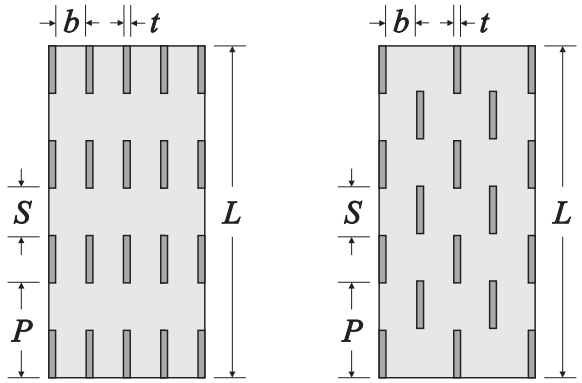

a) Inline Slots b) Staggered Slots

Figure 2: Schematic of Slot Geometry

P/L, and the slot width by the pitch, S/P. The values of these dimensionless parameters vary over the range from 0 to 1:

$$0 < P/L \leq 1, \qquad 0 \leq S/P < 1$$

for the full range of possible slot configurations. Two different slot arrangements, inline and staggered, will be examined in this study as shown in Fig. 2.

The analytical model will assume a uniform velocity of magnitude U through the channels formed between the fins, with no "leakage" of air out the top of the heat sink. This model assumption is valid for shrouded heat sinks, where all the airflow is contained within the channels or for use in conjunction with a flow bypass model for unshrouded heat sinks, such as Wirtz et al. (1994) or Simons and Schmidt (1997).

By assuming that the effects of the baseplate and the shroud can be neglected, the heat sink is modeled as an array of $N-1$ parallel plate channels. This approach is valid in cases where the fin height is much larger than the fin spacing, $H >> b$, such as in the high aspect ratio heat sinks used in power electronics applications. The accuracy of this modeling approach will be reduced when $H \approx b$, where the effects of the baseplate and shroud can no longer be neglected.

The independent and dependent variables are non-dimensionalized using the fin spacing b as the characteristic length. The Reynolds number is defined as:

$$Re_b = \frac{U\,b}{\nu} \tag{1}$$

The average heat transfer rate is non-dimensionalized using the Nusselt number:

$$Nu_b = \frac{Q\,b}{k\,A\,(T_s - T_a)} \tag{2}$$

where T_s and T_a are the source and the inlet air temperatures, respectively, and Q is the total heat transfer rate for a single channel. The total surface area in the channel, A, is determined as a function of the dimensionless slot width:

$$A = 2\,L\,H \cdot \left(1 - \frac{S}{P}\right) \tag{3}$$

All air properties are evaluated at the film temperature:

$$T_f = \frac{T_s + T_a}{2} \tag{4}$$

The analytical models for the slotted fin heat sink will be based on a previously developed modeling procedure for the plate fin heat sink (Teertstra et al., 1999), which will be summarized in the following section.

Plate Fin Heat Sink Model

An analytical model for forced convection cooled plate fin heat sinks has been developed by Teertstra et al. (1999) using the same assumptions presented in the previous section. The model uses a two step procedure that first determines the functional relationship for the average heat transfer coefficient for an isothermal 2D parallel plate channel, and applies this value to a fin analysis to predict the average heat transfer rate for the heat sink.

The first step in the modeling procedure involves the problem of forced convection heat transfer between isothermal parallel plates. Asymptotic solutions for the two limiting cases, fully developed flow and simultaneously developing thermal and hydrodynamic flow, are combined using the inverse formulation of the Churchill and Usagi (1972) composite solution technique:

$$Nu = \left[\left(Nu_{fd}\right)^{-n} + \left(Nu_{dev}\right)^{-n}\right]^{-1/n} \tag{5}$$

The asymptotic solutions for the Nusselt number are presented by Teertstra et al. (1999) as follows:

$$Nu_{fd} = \frac{Re_b^\star\,Pr}{2} \tag{6}$$

$$Nu_{dev} = 0.664\sqrt{Re_b^\star}\,Pr^{1/3}\sqrt{1 + \frac{3.65}{\sqrt{Re_b^\star}}} \tag{7}$$

where the channel Reynolds number, $Re_b^\star$, analogous to the channel, or Elenbaas Rayleigh number in natural convection, is defined as:

$$Re_b^\star = Re_b \cdot \frac{b}{L} \tag{8}$$

Combining the asymptotic solutions using Eq. (5) results in a model for the isothermal parallel plate channel that is valid for the full range of Rayleigh number, as shown in Fig. 3. Using a combination parameter value $n = 3$ the channel model was validated with results from a series of numerical simulations for a wide range of $Re_b^\star$, with a maximum difference of 2% and an RMS difference of less than 1%.

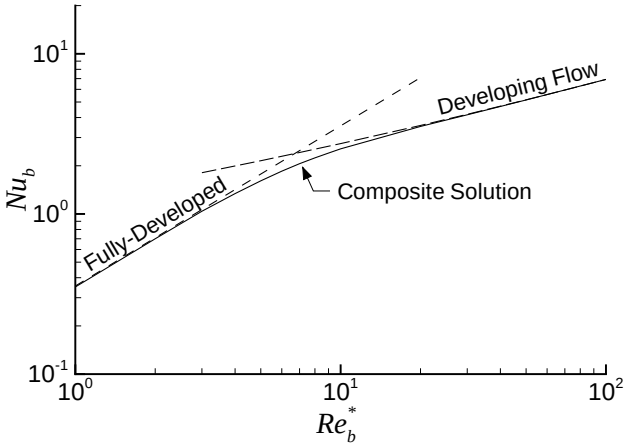

Figure 3: Channel Model Behavior

In most heat sink designs, the goal of maximizing the fin surface area is often achieved at the expense of fin efficiency. Tall, thin fins can lead to increased temperature differences between the fins and baseplate due to increased conductive resistance, and the effectiveness of the fin may be reduced. This effect is most pronounced in forced convection applications, where strong convection from the fins tends to remove heat more quickly than it can be replaced by conduction. In order to apply the parallel plate model to the problem of the plate fin heat sink, the model presented by Teertstra et al. (1999) includes a fin analysis to account for these effects. Treating the isothermal parallel plate channel model as an ideal value, Nu_i, the fin efficiency η is defined by:

$$\eta = \frac{Nu_b}{Nu_i} \tag{9}$$

where Nu_b is the average heat transfer rate for a channel including fin effects. Assuming an adiabatic fin tip condition, the fin efficiency can be determined as a function of the dimensionless parameters:

$$\eta = \frac{\tanh\sqrt{2\,Nu_i\,\frac{k_f}{k}\frac{H}{b}\frac{H}{t}\left(\frac{t}{L}+1\right)}}{\sqrt{2\,Nu_i\,\frac{k_f}{k}\frac{H}{b}\frac{H}{t}\left(\frac{t}{L}+1\right)}} \tag{10}$$

Therefore, for a plate fin heat sink with N fins, the total heat flow rate Q can be determined by:

$$Q = N \cdot \frac{k_f\,A\,(T_s - T_a)}{b} \cdot \eta \cdot Nu_i \tag{11}$$

$$Nu_i = \left[\left(\frac{Re_b^\star Pr}{2}\right)^{-3} + \left(0.664\sqrt{Re_b^\star}Pr^{1/3}\sqrt{1+\frac{3.65}{\sqrt{Re_b^\star}}}\right)^{-3}\right]^{-1/3} \tag{12}$$

Experimental measurements were performed by Teertstra et al. (1999) for an air cooled plate fin heat sink, and the model was found to be in good agreement with the data, within 2.1% RMS difference.

Slotted Heat Sink Models

Unlike the plate fin heat sink, where clearly defined limiting cases with asymptotic solutions exist, the slotted fin heat sink is a complex problem for which exact solutions are not possible. However, based on the model for the plate fin heat sink it is possible to derive models for the upper and lower bounds on the solution. These bounds are defined as the solutions to geometrically-similar problems that provide upper and lower limits for the results, and all data for a particular heat sink configuration will fall between these bounds.

The original premise for the use of slotted fins was that new thermal boundary layers would be initiated at each fin section, thereby reducing the average boundary layer thickness and increasing the average heat transfer coefficient. Lower and upper bounds for the thermal performance of the heat sink are defined based on two limiting cases for the boundary layer growth. The lower bound corresponds to the situation where no new thermal boundary layers are formed, resulting in thicker boundary layers and lower average heat transfer coefficient values. The upper bound is achieved when new thermal and hydrodynamic boundary layers are initiated at each fin section, independent of any upstream effects. Models for the lower and upper bounds, based on the plate fin heat sink model, will be developed in the following sections.

Lower Bound

The lower bound on the average heat transfer for the slotted fin heat sink has been described as occurring when no new thermal boundary layers are formed in the channels between the fins. This lower bound

is modeled by an equivalent channel with length L_{LB} corresponding to the combined length of all the fin sections, as shown in Fig. 4. This lower bound fin length can be determined by:

$$L_{LB} = L - N_S \cdot S \tag{13}$$

where N_S is the number of slots in the fins. In the case of staggered slot arrangement, L_{LB} can be determined by averaging the total fin section lengths on each side of the channel, as shown in Fig. 4b). For long heat sinks where $P << L$, the number of slots can be approximated by $N_S = L/P$, which leads to the following expression for the lower bound length:

$$L_{LB} = L\left(1 - \frac{S}{P}\right) \tag{14}$$

Based on this new, lower bound length, two parameters in the plate fin heat sink model will be modified:

$$Re^{\star}_{LB} = \frac{Re^{\star}_{b}}{1 - S/P} \tag{15}$$

$$\frac{t}{L_{LB}} = \frac{t/L}{1 - S/P} \tag{16}$$

Substituting these lower bound expressions into the plate fin heat sink model gives the following:

$$Nu_{LB} = \eta_{LB} \cdot Nu_i \tag{17}$$

$$\eta_{LB} = \frac{\tanh\sqrt{2\,Nu_i\,\frac{k_f}{k}\frac{H}{b}\frac{H}{t}\left(\frac{\frac{t}{L}}{1-\frac{S}{P}}+1\right)}}{\sqrt{2\,Nu_i\,\frac{k_f}{k}\frac{H}{b}\frac{H}{t}\left(\frac{\frac{t}{L}}{1-\frac{S}{P}}+1\right)}} \tag{18}$$

$$Nu_i = \left[\left(\frac{Re^{\star}_{LB}Pr}{2}\right)^{-3} + \left(0.664\sqrt{Re^{\star}_{LB}}Pr^{1/3}\sqrt{1+\frac{3.65}{\sqrt{Re^{\star}_{LB}}}}\right)^{-3}\right]^{-1/3} \tag{19}$$

Upper Bound

Unlike the lower bound, which assumes that no new boundary layers were formed as a result of the slots, the upper bound model assumes the best possible case,

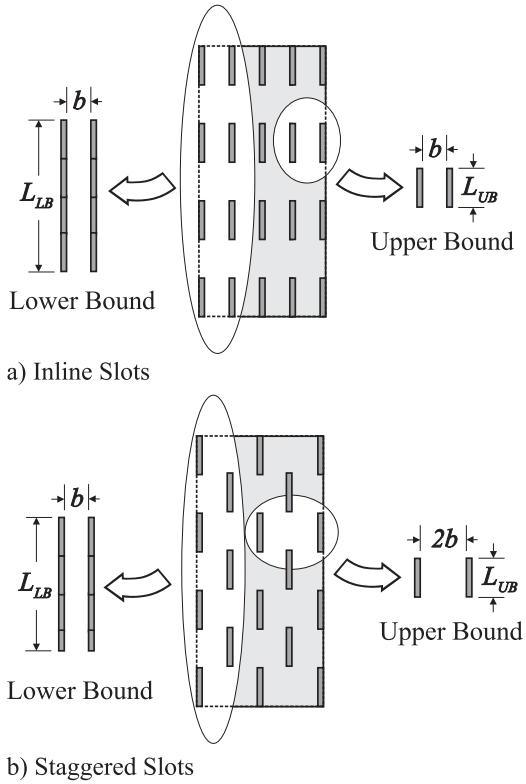

Figure 4: Schematic of Lower and Upper Bound Models

that a new boundary layer forms at each fin section independent of any upstream effects. This bound is modeled by focusing on the channel formed between two fin sections, as shown in Fig. 4. The length of this equivalent channel, L_{UB}, corresponds to the length of a single fin section:

$$L_{UB} = P - S \tag{20}$$

When expressed in terms of the previously defined dimensionless slot pitch and width, this upper bound length becomes:

$$L_{UB} = L\left(\frac{P}{L}\right)\left(1 - \frac{S}{P}\right) \tag{21}$$

For inline slots the fin spacing b is used in the upper bound model, while for staggered slots the width of the equivalent channel is equal to $2b$.

As in the lower bound model, the two parameters in the heat sink model that depend on the fin length are modified as follows:

$$Re^{\star}_{UB} = \frac{Re^{\star}_{b}}{P/L\,(1 - S/P)} \tag{22}$$

$$\frac{t}{L_{UB}} = \frac{t/L}{P/L\,(1 - S/P)} \tag{23}$$

Substituting these upper bound parameters into the heat sink model gives the following expressions for the upper bound for the inline slot arrangement:

$$Nu_{UB} = \eta_{UB} \cdot Nu_i \tag{24}$$

$$\eta_{UB} = \frac{\tanh\sqrt{2\,Nu_i\,\frac{k_f}{k}\frac{H}{b}\frac{H}{t}\left(\frac{\frac{t}{L}}{\frac{P}{L}\left(1-\frac{S}{P}\right)}+1\right)}}{\sqrt{2\,Nu_i\,\frac{k_f}{k}\frac{H}{b}\frac{H}{t}\left(\frac{\frac{t}{L}}{\frac{P}{L}\left(1-\frac{S}{P}\right)}+1\right)}} \tag{25}$$

$$Nu_i = \left[\left(\frac{Re^{\star}_{UB}Pr}{2}\right)^{-3} + \left(0.664\sqrt{Re^{\star}_{UB}}Pr^{1/3}\sqrt{1+\frac{3.65}{\sqrt{Re^{\star}_{UB}}}}\right)^{-3}\right]^{-1/3} \tag{26}$$

The upper bound model for the staggered fin arrangement is determined in a similar fashion by substituting $2b$ for the channel width in Eqs. (24 - 26).

EXPERIMENTAL MEASUREMENTS

Experimental tests were performed to validate the proposed bounds models using commercially-available heat sink prototypes with a variety of slot pitches and widths, as summarized in Table 1.

Matching pairs of heat sinks were fastened together in a back-to-back arrangement, and two 300 W pencil heaters were press-fit into holes drilled at the interface between the baseplates. Given the symmetry of this configuration, it is assumed that all the heat dissipated by the heaters was equally distributed between the two heat sinks.

Temperature measurements were performed using 5 *mil* T-type copper-constantan thermocouples connected to a Fluke Helios datalogger. Baseplate temperatures were measured using 4 thermocouples attached to the baseplate of one of the heat sinks at the locations indicated by T_1 - T_4 indicated in Fig. 5. These thermocouples were located close to and far away from the heaters, such that an arithmetic average of their measured values would provide a representative value for the average baseplate temperature T_s. The maximum difference noted between the thermocouple readings during the tests was less than 15% of the average temperature, validating the assumption of a uniform baseplate temperature.

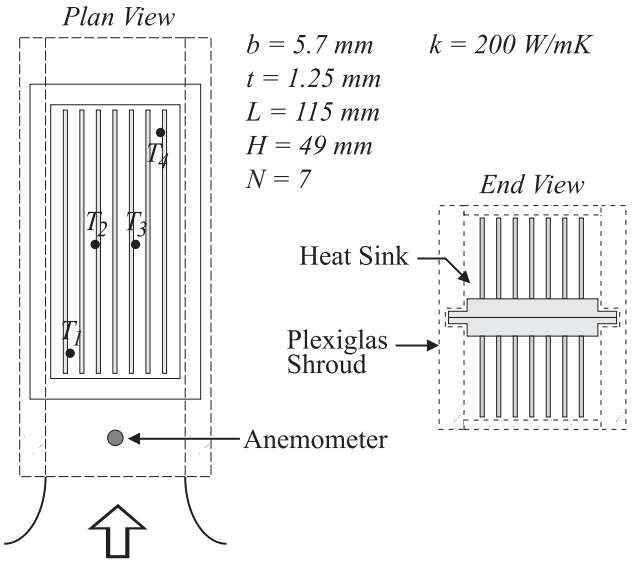

Figure 5: Schematic of Experimental Apparatus

Table 1: Summary of Experimental Tests

Test	P/L	S/P	Slot Arrangement
1	0.059	0.54	Inline
2	0.11	0.5	Inline
3	0.22	0.5	Inline
4	0.44	0.5	Inline
5	0.22	0.5	Staggered
6	0.44	0.5	Staggered

To minimize flow bypass effects the heat sink assembly was placed inside a Plexiglas shroud, as shown in Fig. 5. The inner dimensions of the shroud were within one channel of each of the sides of the heat sink, and the baseplate edges were narrowed to reduce conduction losses to the shroud. The shroud and heat sink assembly were suspended in the center of a $300\,mm \times 300\,mm$ test section of a vertical, open-circuit wind tunnel, and the spaces between the shroud and the test section were filled to prevent bypass. Velocities were measured approximately $200\,mm$ upstream of the heat sink using a Dantec hot wire anemometer, as shown in Fig. 5.

Tests were performed at one power level, $Q = 500W$, for a range of approach velocity values, $U_a = 2, 3, 4, 5, 6, 7, 8\,m/s$. Each test was allowed to reach steady-state over a 3 - 4 hour period, and the results were recorded when the measured values remained unchanged for a 15 minute period.

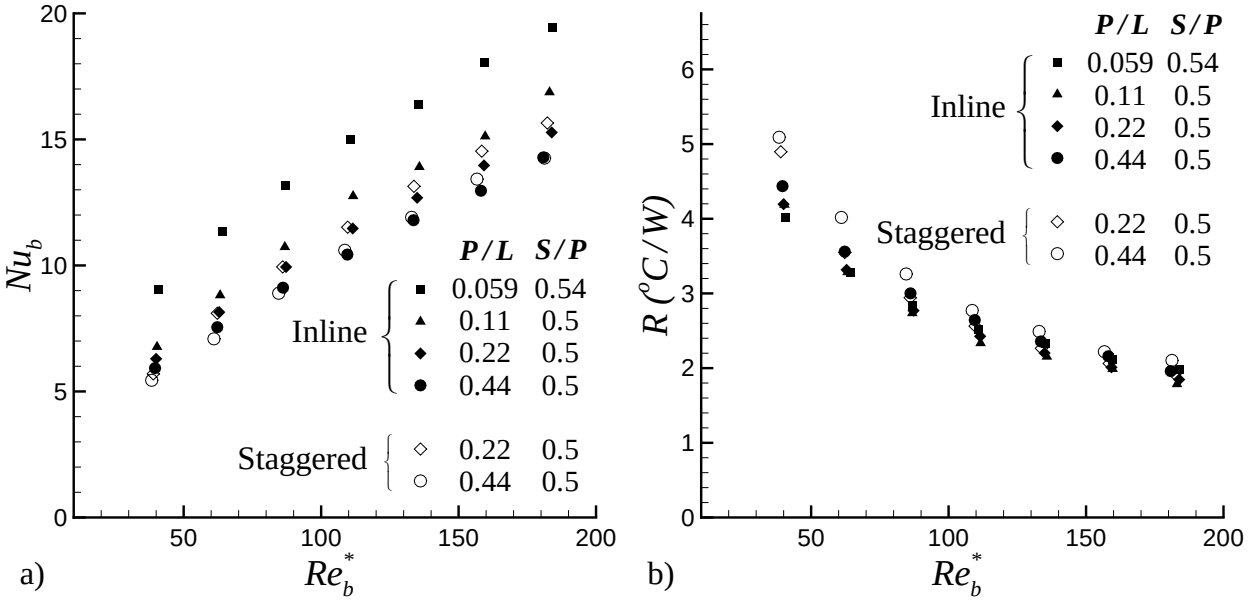

Figure 6: Experimental Measurements for Slotted Heat Sinks: a) Nu_b vs. $Re_b^\star$; b) R vs. $Re_b^\star$

Radiation tests were performed for each of the heat sink prototypes in a vacuum environment and the results were used to reduce radiation effects from the convective tests. In all cases, the relative magnitude of the radiative component was less than 1% of the total heat transfer, as expected in forced convection applications.

In order to compare the measured values with the predictions of the bounds models, they must be converted in terms of the previously defined dimensionless parameters, $Re_b^\star$ and Nu_b. By a simple continuity relationship the average velocity in the channels formed between the heat sink fins is related to the approach velocity:

$$U = \frac{A_a}{A_o}\, U_a \tag{27}$$

where A_a and A_o are the cross sectional areas of the inlet and heat sink sections, respectively. The resulting channel velocity can be expressed in terms of the Reynolds number defined in Eq. (1), where the properties are evaluated at the film temperature.

The total heat transfer rate, Q, (less radiation) is divided by the total number of channels per side, N, which includes the two half channels formed between the outer fins and the shroud, to give the per-channel heat transfer rate. This value is non-dimensionalized by the previously defined Nusselt number:

$$Nu_b = \frac{\left(\dfrac{Q/2}{N}\right) b}{k\, A\, \Delta T} \tag{28}$$

In order to examine the balance between the convection enhancement of the slots and the reduction in surface area an additional dependent variable, the thermal resistance R, is defined:

$$R = \frac{1}{h\, A} \tag{29}$$

where h is the average heat transfer coefficient, which can be related to the Nusselt number by its definition:

$$Nu_b = \frac{h\, b}{k}$$

The experimental data are plotted in Fig. 6 for all slot configurations and Reynolds numbers examined in the current study. Figure 6 a) presents the Nusselt number vs. $Re_b^\star$ for the 4 inline and 2 staggered slot configurations for the range of Reynolds number $40 \le Re_b^\star \le 180$. The data in Fig. 6 a) indicates that a decrease in the slot pitch and an increase in the slot size contributes to a substantial increase in the Nusselt number. For the slot configuration $P/L = 0.059$, $S/P = 0.54$, the Nu_b is approximately 30% higher than for any of the remaining cases, $P/L \ge 0.11$, $S/P = 0.5$, for the full range of $Re_b^\star$. For the fin spacings and slot pitches tested, staggering the slots had only a small effect on the average results.

MODEL VALIDATION

The proposed models for the lower and upper bounds on the average Nusselt number for the slotted fin heat sink are compared with the experimental data in Fig. 7 a) - f). In all of the cases reported in Fig. 7 the data are contained within the upper and

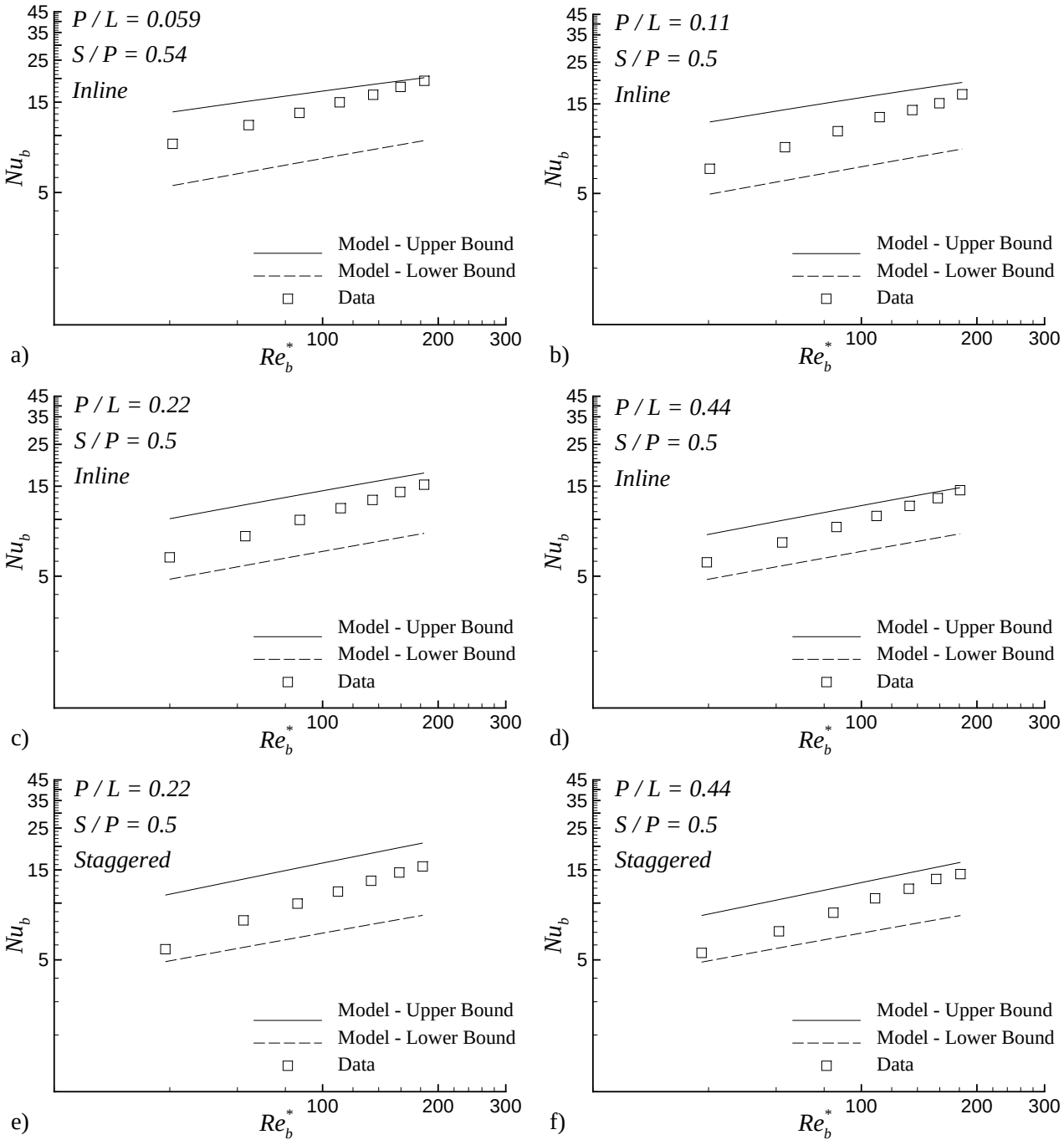

Figure 7: Comparison of Bounds with Experimental Data

lower limits for the full range of $Re_b^\star$. For each of the slot configurations tested the data moves smoothly between the limits, from the lower bound for small $Re_b^\star$ to the upper bound for large $Re_b^\star$. For small P/L values and larger values of S/P, such as in Fig. 7 a) the data tends towards the upper bound with each fin section acting independently, and there is a significant difference between the bounds. For large P/L and small values of S/P, such as shown in Fig. 7 d) and f), the difference between the lower and upper bounds, and the data approaches both limits for the range of $Re_b^\star$ tested. Figure 7 also shows that there is little difference between the inline and staggered slot arrangements for the range of configurations tested.

The current bounds models can be used to formulate a design tool to predict slotted heat sink perfor-

mance for the range of slot configurations examined in this study, $0.11 \leq P/L \leq 0.44$ and $S/P = 0.5$. For this range of values, the average Nusselt number can be approximated by the arithmetic mean of the lower and upper bounds:

$$Nu_b = \frac{Nu_{LB} + Nu_{UB}}{2} \tag{30}$$

which results in an RMS percent difference of 12% for the range of channel Reynolds number: $40 \leq Re_b^\star \leq 180$. For $Re_b^\star > 180$ or $P/L < 0.1$ the upper bound model should be used to predict the average Nusselt number, $Nu_b = Nu_{UB}$.

Because of the limited range of S/P values in the current data it is difficult to formulate a reliable procedure to predict optimal slot pitch and width as a function of $Re_b^\star$ and the surface area A. As shown in Figs. 6 a) and b), the thermal performance of a slotted heat sink depends on both the enhancement of the heat transfer and the reduction in surface area, and the prediction of the "best" values of P/L and S/P may change as a function of $Re_b^\star$. Additional study and experimental data for other values of S/P are required to develop a general procedure for optimizing slot size and pitch that is applicable to the full range of the independent parameters.

SUMMARY AND CONCLUSIONS

Models for the lower and upper bounds on the average dimensionless heat transfer coefficient for slotted fin heat sinks have been developed. Experimental measurements have been performed for a range of slot configurations, $S/P \approx 0.5$, $0.059 \leq P/L \leq 0.44$, for the range of Reynolds number, $40 \leq Re_b^\star \leq 180$. The data has been shown to lie within the proposed bounds for the full range of test conditions, with the data moving smoothly from the lower to upper limits. An approximate model for predicting the performance of slotted fin heat sinks based on an arithmetic mean of the bounds has been proposed, with an RMS percent difference from the model of 12%. The need for additional data to develop a general method suitable for the optimization of the slot size and pitch as a function of the independent parameters has been identified.

ACKNOWLEDGMENTS

The authors gratefully acknowledge the continued financial support of R-Theta Inc. and Materials and Manufacturing Ontario.

REFERENCES

R-Theta Inc., 1999, 6220 Kestrel Rd., Mississauga, ON, L5T 1Y9, Canada, through personal communication.

Teertstra, P., Yovanovich, M.M., Culham, J.R and Lemczyk, T.F., 1999, "Analytical Forced Convection Modeling of Plate Fin Heat Sinks," *15th Annual IEEE Semiconductor Thermal Measurement and Management Symposium,* San Diego, CA, March 9 - 11, pp. 34 - 41.